General formulation for light scattering by a dielectric body near a perfectly conducting surface

J. C. Chao, F. J. Rizzo, I. Elshafiey, Y. J. Liu, L. Upda, and P. A. Martin*

Iowa State University, Ames, Iowa 50011

Received March 27, 1995; revised manuscript received June 26, 1995; accepted August 8, 1995

We present an efficient approach for calculating the electromagnetic scattered fields (light) from a single dielectric body situated above a perfectly conducting (or reflecting) half-space. This approach employs the boundary integral equation method and is applicable to arbitrarily shaped scatterers located anywhere above the conducting half-space surface, impinged upon by arbitrary incident fields. Numerical results for spherical scatterers are presented and are compared with published results obtained with an analytical approach.

1. INTRODUCTION

Problems involving light scattered from particles on or near a perfectly conducting surface have been the topic of extensive research, both theoretically and experimentally, for many years. This research is motivated by the need to study problems caused by particle contamination in optical systems. Often particle contamination causes system degradation as well as local heating problems.[1,2] The accurate modeling of the scattered light, or of electromagnetic (EM) fields in general, can provide significant insight into the properties of the particles as well as into the extent of system degradation.

Examples of previous analytical work, both approximate and exact, on such problems include a formulation involving the combination of the multipole-expansion method and image theory (IT).[2] This formulation was developed to solve exactly for the EM scattered fields from a dielectric sphere near a perfectly conducting plane surface impinged upon by a normally incident plane wave. A similar approach was also taken in Ref. 3, in which an extension to the Mie theory was employed to calculate Müeller scattering matrices for spherical scatterers above a half-plane surface. In Ref. 4, analytic solutions for spheres near a half-space were obtained by application of the Lorentz–Mie scattering theory along with the Debye-potential method. All of these methods, however, are limited to spherical scatterers or other canonical-shaped scatterers. For solving the scattered fields from arbitrarily shaped scatterers near a surface, Lindell *et al.*[5] developed an approximate method utilizing the exact image theory, in which the scatterer is assumed to be small compared with the incident wavelength and far away from the half-space, so the internal field can be treated as a uniform plane wave. A compromise approach to modeling the scatterer/surface problem is to assume that the scattered waves consist of rays that are reflected off the surface either before or after interacting with the scatterer.[1,6,7]

Practically, contaminant particles are not always spherical in shape. Consequently, methods capable of calculating the scattered fields from arbitrarily shaped particles are needed. Boundary integral equation (BIE) methods are well suited for calculating the EM scattered fields from arbitrarily shaped scatterers. In particular, they are most effective for homogeneous and bounded scatterers where the integration (consequently, the discretization) process is over only the finite bounding surface of the scatterers. This situation can be seen in the literature where BIE methods have been applied successfully to both single-scattering and multiple-scattering problems.[8–11] In addition, BIE methods can be applied to problems involving unbounded scatterers with an indefinite-sized surface by modification of the Green function, otherwise known as the kernel function, in the integral equation. If this modified Green function is used, no discretization (or truncation) of the indefinite-sized surface is needed. For example, in the case of a flat half-space surface, the modified Green function (half-space Green function) consists of the free-space Green function plus an additional function to account for the presence of the half-space. However, this additional function is quite complicated for a dielectric half-space, where it requires the evaluation of integrals over infinite wave numbers. This evaluation often presents numerical difficulties, such as instability, during the implementation stage. Use of this function is computationally intensive and is not always a fair trade in efficiency compared with discretizing a truncated half-space surface. Nevertheless, for the case of scatterers situated near a perfectly conducting half-space, the modified Green function is simple and can be easily computed if the singularities inherent in the governing integral equations are treated properly.

The objective of this paper is to present a more general approach for solving EM scattering problems involving arbitrarily shaped scatterers near a perfectly conducting surface with arbitrary incident fields. This more general approach employs the BIE method with the well-known modified Green function to account for the perfectly conducting half-space. The modified Green function can be easily derived by application of IT to the formulation for two-scatterer problems. The most general form of the modified Green function for a dielec-

0740-3232/96/020338-07$06.00

tric half-space is shown in Eq. (2.3.5) of Ref. 12. To obtain the modified Green function for the simpler case of a perfectly conducting half-space, one can set the reflection coefficient $\tilde{R}_{12}^{\mathrm{TM}} = 1$ to account for total reflection and then apply Eq. (2.2.31) of Ref. 12 to get a closed-form expression.

The BIE formulation is valid for arbitrarily shaped scatterers located anywhere above the perfectly conducting half-space, but in this preliminary paper all validation work was done with spherical scatterers. This choice was made because we wish to check first with analytical results, and these are readily available for spherical scatterers. In addition, we have computed scattering cross sections for several ellipsoidal scatterers, which resemble more closely the actual shape of dust contaminants. However, it should be emphasized that no advantages in the analytical formulation or in the computer implementation were found when these geometries were used. Consequently, further numerical simulations can and will be performed with the same model for arbitrarily shaped scatterers above a perfectly conducting surface, and the results will be compared with data taken from physical experiments; we expect to report our findings subsequently.

2. IMAGE THEORY

In the EM theory, a BIE formulation for scattering problems is one that deals with integrals of unknown equivalent current densities multiplied by Green functions. The integrals are over the bounding surfaces of the objects. These integrals give the electromagnetic fields both internal and external to the scatterer. For the problem of dielectric scatterers near a perfectly conducting half-space, these equivalent currents can be viewed as actual sources above the half-space. Then by application of IT, the perfectly conducting half-space is replaced by a set of virtual sources existing on a virtual scatterer located below the half-space. The scattering problem to be solved is shown in Fig. 1, where a dielectric scatterer is situated near a perfectly conducting half-plane with a plane incident wave propagating toward the half-space. The equivalent problem produced by the application of IT is shown in Fig. 2, where a set of equivalent sources at the imaged location of the original scatterer that represents the half-space surface is explicitly introduced. A reflected plane wave with the same magnitude as the incident plane wave is also shown. The polarization of the reflected wave is such that the boundary condition ($\vec{E} = 0$) at the half-space interface is satisfied.

More generally, virtual sources are such that when combined with the real sources, they form an equivalent system that replaces the original system. In effect, virtual sources account for the presence of the perfectly conducting half-space. Consider Fig. 3, which contains both real and virtual sources.[13] However, the equivalent system gives a meaningful solution only above but not below the conducting plane, where the field is actually zero.

3. PROBLEM FORMULATION

We start out by considering the most general form of electromagnetic integral equations for a two-scatterer problem as given in Eqs. (1)–(4) (see Ref. 16):

$$\begin{aligned}
&\nabla_P \times \int_{S_k} (\hat{n} \times \vec{E})_k(q) G_e(P, q)\mathrm{d}S_q \\
&\quad + \frac{j}{\omega \epsilon_e} \nabla_P \times \nabla_P \times \int_{S_k} (\hat{n} \times \vec{H})_k(q) G_e(P, q)\mathrm{d}S_q \\
&\quad + \nabla_P \times \int_{S_j} (\hat{n} \times \vec{E})_j(q) G_e(P, q)\mathrm{d}S_q \\
&\quad + \frac{j}{\omega \epsilon_e} \nabla_P \times \nabla_P \times \int_{S_j} (\hat{n} \times \vec{H})_j(q) G_e(P, q)\mathrm{d}S_q \\
&\qquad = \begin{cases} \vec{E}_e(P) & P \in \text{ exterior} \\ -\vec{E}_{\mathrm{inc}}(P) & P \in \text{ interior of } S_k \end{cases}, \qquad (1)
\end{aligned}$$

$$\begin{aligned}
&\nabla_P \times \int_{S_k} (\hat{n} \times \vec{H})_k(q) G_e(P, q)\mathrm{d}S_q \\
&\quad - \frac{j}{\omega \mu_e} \nabla_P \times \nabla_P \times \int_{S_k} (\hat{n} \times \vec{E})_k(q) G_e(P, q)\mathrm{d}S_q \\
&\quad + \nabla_P \times \int_{S_j} (\hat{n} \times \vec{H})_j(q) G_e(P, q)\mathrm{d}S_q \\
&\quad - \frac{j}{\omega \mu_e} \nabla_P \times \nabla_P \times \int_{S_j} (\hat{n} \times \vec{E})_j(q) G_e(P, q)\mathrm{d}S_q \\
&\qquad = \begin{cases} \vec{H}_e(P) & P \in \text{ exterior} \\ -\vec{H}_{\mathrm{inc}}(P) & P \in \text{ interior of } S_k \end{cases}, \qquad (2)
\end{aligned}$$

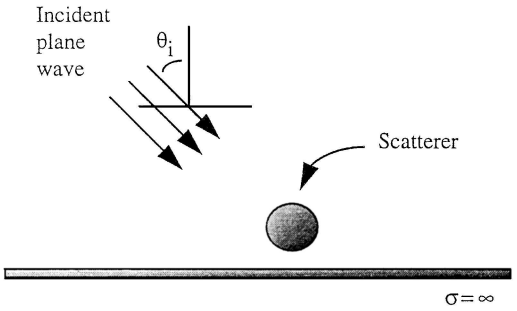

Fig. 1. Sample scattering problem of a dielectric object near a perfectly conducting half-space.

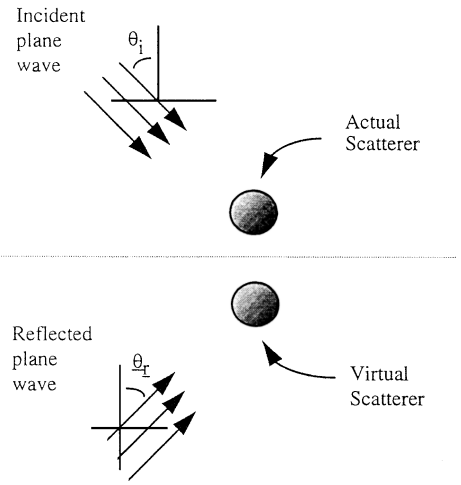

Fig. 2. Recasting the original problem into a two-scatterer problem by application of the image theory.

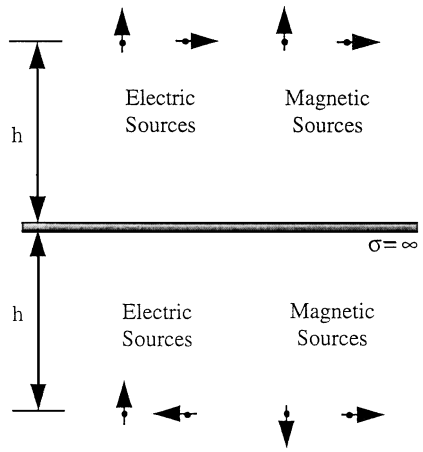

Fig. 3. Image theory illustrating the real and virtual sources for both electric and magnetic sources.

$$\nabla_P \times \int_{S_k} (\hat{n} \times \vec{E})_k(q) G_{ik}(P, q) \mathrm{d}S_q + \frac{j}{\omega \epsilon_{ik}} \nabla_P \times \nabla_P \times \int_{S_k} (\hat{n} \times \vec{H})_k(q) G_{ik}(P, q) \mathrm{d}S_q = \begin{cases} 0 & P \in \text{ exterior} \\ -\vec{E}_i(P) & P \in \text{ interior of } S_k \end{cases}, \quad (3)$$

$$\nabla_P \times \int_{S_k} (\hat{n} \times \vec{H})_k(q) G_{ik}(P, q) \mathrm{d}S_q - \frac{j}{\omega \mu_{ik}} \nabla_P \times \nabla_P \times \int_{S_k} (\hat{n} \times \vec{E})_k(q) G_{ik}(P, q) \mathrm{d}S_q = \begin{cases} 0 & P \in \text{ exterior} \\ -\vec{H}_i(P) & P \in \text{ interior of } S_k \end{cases}. \quad (4)$$

The subscripts j and k represent the scatterer of interest (i.e., 1 or 2); but $j \neq k$, e and i represent the region exterior and interior, respectively, to that scatterer and inc represents the incident field impinging on the scatterers. The point P is a field point located in either region e or region i, and the point q is an integration point located on the scatterer surface. In Eqs. (1)–(4) the integration takes place over both surfaces, $\hat{n}$ is the outward-pointing unit normal, G_α is the free-space Green function,

$$G_\alpha(p, q) = \frac{\exp(k_\alpha |p - q|)}{4\pi |p - q|}, \quad (5)$$

and ω is the radial frequency of the incident field. The subscript α is either e or i. The quantities ϵ, μ, and k represent, respectively, the permittivity, permeability, and wave number of the appropriate region. In addition, the tangential interface conditions shown in Eqs. (6)–(9) have been enforced. Therefore, to calculate the scattered fields in either the exterior or the interior region, one needs first to solve the tangential surface fields on all scatterers and then substitute these values back into Eqs. (1)–(4). To calculate the surface fields, we define a set of equivalent current densities, using the tangential surface fields, and take the limit as the field point P (in e or i) moves to a point p on the scatterer surface. The unknowns $\vec{J}$ and $\vec{M}$ represent the equivalent surface electric and magnetic current densities, respectively.

$$\hat{n}_1 \times \vec{E} = \hat{n}_1 \times \vec{E}_1 = -\vec{M}_1, \quad (6)$$

$$\hat{n}_1 \times \vec{H} = \hat{n}_1 \times \vec{H}_1 = \vec{J}_1, \quad (7)$$

$$\hat{n}_2 \times \vec{E} = \hat{n}_2 \times \vec{E}_1 = -\vec{M}_2, \quad (8)$$

$$\hat{n}_2 \times \vec{H} = \hat{n}_2 \times \vec{H}_1 = \vec{J}_2. \quad (9)$$

The problem of a single scatterer above a perfectly conducting surface is similar to the above two-scatterer problem[9] but with two different incident fields: the first is a plane wave originating from the upper half-space, and the second is an equivalent reflected plane wave that is a direct consequence of the presence of the half-space.[2] The polarization of the reflected wave is such that the electric field is zero and the magnetic field is twice the incident field at the half-space surface. The size of the system to be solved, however, is only one half of the system size of the two-scatterer case, owing to the application of the IT. This reduction in system size can be observed from the conditions imposed in Fig. 3.

There are two approaches that one can take to solve this problem. First, one can account for the difference in signs by modifying the free-space Green function to reflect sign changes dealing with each of the three components of the equivalent currents. An alternative approach will allow the use of the free-space Green function as if the problem were a two-scatterer problem. Then one reduces the system of equations by combining equations as dictated by the appropriate sign differences. In this paper we choose the latter approach so that the multiple-scattering computer program that we developed in Ref. 9 can be readily used without significant modifications. However, one can also adopt the first approach and obtain identical results.

The governing BIE's for the present problem are identical to the BIE's for the two-body scattering problem except that the collocation process needs to take place only on either the top scatterer or the bottom scatterer but not on both. In this paper we choose to collocate on the top scatterer. To obtain the governing BIE's, we start from Eqs. (1)–(4) and take the limit as P approaches a surface point p. Next we take the cross product between the unit normal at p and the resulting equations. We define the bounding surfaces of the top scatterer to be S_1 and the bottom scatterer to be S_2, and the governing BIE's are as follows:

for $p \in S_1$,

$$\tfrac{1}{2}\vec{M}_1(p) - \hat{n}_{1p} \times \nabla_p \times \int_{S_1} \vec{M}_1(q) G_e(p, q) \mathrm{d}S_q + \frac{j}{\omega \epsilon_e} \hat{n}_{1p} \times \nabla_p \times \nabla_p \times \int_{S_1} \vec{J}_1(q) G_e(p, q) \mathrm{d}S_q - \hat{n}_{1p} \times \nabla_p \times \int_{S_2} \vec{M}_2(q) G_e(p, q) \mathrm{d}S_q + \frac{j}{\omega \epsilon_e} \hat{n}_{1p} \times \nabla_p \times \nabla_p \times \int_{S_2} \vec{J}_2(q) G_e(p, q) \mathrm{d}S_q = -\hat{n}_{1p} \times [\vec{E}_{\text{inc}}(p) + \vec{E}_{\text{ref}}(p)], \quad (10)$$

$$
\begin{aligned}
&\tfrac{1}{2}\vec{J}_1(p) - \hat{n}_{1p} \times \nabla_p \times \int_{S_1} \vec{J}_1(q) G_e(p, q) \mathrm{d}S_q \\
&\quad - \frac{j}{\omega \mu_e} \hat{n}_{1p} \times \nabla_p \times \nabla_p \times \int_{S_1} \vec{M}_1(q) G_e(p, q) \mathrm{d}S_q \\
&\qquad - \hat{n}_{1p} \times \nabla_p \times \int_{S_2} \vec{J}_2(q) G_e(p, q) \mathrm{d}S_q \\
&\quad - \frac{j}{\omega \mu_e} \hat{n}_{1p} \times \nabla_p \times \nabla_p \times \int_{S_2} \vec{M}_2(q) G_e(p, q) \mathrm{d}S_q \\
&\qquad = \hat{n}_{1p} \times [\vec{H}_{\mathrm{inc}}(p) + \vec{H}_{\mathrm{ref}}(p)], \quad (11)
\end{aligned}
$$

$$
\begin{aligned}
&\tfrac{1}{2}\vec{M}_1(p) + \hat{n}_{1p} \times \nabla_p \times \int_{S_1} \vec{M}_1(q) G_i(p, q) \mathrm{d}S_q \\
&\quad - \frac{j}{\omega \epsilon_i} \hat{n}_{1p} \times \nabla_p \times \nabla_p \times \int_{S_1} \vec{J}_1(q) G_i(p, q) \mathrm{d}S_q = 0, \quad (12)
\end{aligned}
$$

$$
\begin{aligned}
&\tfrac{1}{2}\vec{J}_1(p) + \hat{n}_{1p} \times \nabla_p \times \int_{S_1} \vec{J}_1(q) G_i(p, q) \mathrm{d}S_q \\
&\quad + \frac{j}{\omega \mu_i} \hat{n}_{1p} \times \nabla_p \times \nabla_p \times \int_{S_1} \vec{M}_1(q) G_i(p, q) \mathrm{d}S_q = 0. \quad (13)
\end{aligned}
$$

If one chooses to collocate on the bottom scatterer, Eqs. (10)–(14) still hold except that the subscripts 1 and 2 need to be interchanged. To avoid the spurious resonance problem[15] and to reduce the hypersingular integrals into weakly singular integrals,[16] we adopt the Müller formulation. For a detailed discussion on the singularity issues associated with the BIE method, Refs. 9 and 16 provide an extensive analysis on the regularization of singular integrals into regular integrals so that the integrals can be computed numerically. The resulting linear combinations are

$$
\begin{aligned}
&\epsilon_e \Bigg[\tfrac{1}{2}\vec{M}_1(p) - \hat{n}_{1p} \times \nabla_p \times \int_{S_1} \vec{M}_1(q) G_e(p, q) \mathrm{d}S_q + \frac{j}{\omega \epsilon_e} \hat{n}_{1p} \times \nabla_p \times \nabla_p \times \int_{S_1} \vec{J}_1(q) G_e(p, q) \mathrm{d}S_q \\
&\qquad - \hat{n}_{1p} \times \nabla_p \times \int_{S_2} \vec{M}_2(q) G_e(p, q) \mathrm{d}S_q + \frac{j}{\omega \epsilon_e} \hat{n}_{1p} \times \nabla_p \times \nabla_p \times \int_{S_2} \vec{J}_2(q) G_e(p, q) \mathrm{d}S_q \Bigg] \\
&\qquad - \epsilon_i \Bigg[\tfrac{1}{2}\vec{M}_1(p) + \hat{n}_{1p} \times \nabla_p \times \int_{S_1} \vec{M}_1(q) G_i(p, q) \mathrm{d}S_q - \frac{j}{\omega \epsilon_{i1}} \hat{n}_{1p} \times \nabla_p \times \nabla_p \times \int_{S_1} \vec{J}_1(q) G_i(p, q) \mathrm{d}S_q \Bigg] \\
&\qquad = \epsilon_e \{ -\hat{n}_{1p} \times [\vec{E}_{\mathrm{inc}}(p) + \vec{E}_{\mathrm{ref}}(p)] \}, \quad (14)
\end{aligned}
$$

$$
\begin{aligned}
&\mu_e \Bigg[\tfrac{1}{2}\vec{J}_1(p) - \hat{n}_{1p} \times \nabla_p \times \int_{S_1} \vec{J}_1(q) G_e(p, q) \mathrm{d}S_q - \frac{j}{\omega \mu_e} \hat{n}_{1p} \times \nabla_p \times \nabla_p \times \int_{S_1} \vec{M}_1(q) G_e(p, q) \mathrm{d}S_q \\
&\qquad - \hat{n}_{1p} \times \nabla_p \times \int_{S_2} \vec{J}_2(q) G_e(p, q) \mathrm{d}S_q - \frac{j}{\omega \mu_e} \hat{n}_{1p} \times \nabla_p \times \nabla_p \times \int_{S_2} \vec{M}_2(q) G_e(p, q) \mathrm{d}S_q \Bigg] \\
&\qquad - \mu_i \Bigg[\tfrac{1}{2}\vec{J}_1(p) + \hat{n}_{1p} \times \nabla_p \int_{S_1} \vec{J}_1(q) G_i(p, q) \mathrm{d}S_q + \frac{j}{\omega \mu_{i1}} \hat{n}_{1p} \times \nabla_p \times \nabla_p \times \int_{S_1} \vec{M}_1(q) G_i(p, q) \mathrm{d}S_q \Bigg] \\
&\qquad = \mu_e \{ \hat{n}_{1p} \times [\vec{H}_{\mathrm{inc}}(p) + \vec{H}_{\mathrm{ref}}(p)] \}. \quad (15)
\end{aligned}
$$

Equations (14) and (15) constitute a set of BIE's that are uniquely solvable at all frequencies. To solve for the unknown current densities on the surfaces, one must first transform the continuous BIE's into discrete linear systems of equations by discretizing the integration surfaces into a set of surface elements (or patches) with a fixed number of nodes on each element. The unknown current densities to be solved are defined only at the nodes. The current densities and the geometrical information at other locations on the element are obtained by interpolation with use of the nodal unknowns and a set of quadratic basis functions as shown in Eqs. (16)–(18):

$$
x_k = \sum_{\beta=1}^{m} N^{\beta} x_k{}^{\beta}, \quad (16)
$$

$$
M_k = \sum_{\beta=1}^{m} N^{\beta} M_k{}^{\beta}, \quad (17)
$$

$$
J_k = \sum_{\beta=1}^{m} N^{\beta} J_k{}^{\beta}. \quad (18)
$$

Here k represents the kth tangential component in the local coordinate system[16] ($k = 1, 2$), m is the number of nodes on an element, β is the nodal index on the element, and N^{β} is the basis function associated with node β. Substituting Eqs. (16)–(18) into Eqs. (14) and (15) results in a set of linear equations with the unknown vector containing the nodal current densities on both surfaces:

$$
\begin{aligned}
&\begin{bmatrix} \mathbf{A}_{11} & \mathbf{A}_{12} & \mathbf{A}_{13} & \mathbf{A}_{14} \\ \mathbf{A}_{21} & \mathbf{A}_{22} & \mathbf{A}_{23} & \mathbf{A}_{24} \end{bmatrix} \begin{bmatrix} \mathbf{M}_k{}^{a} \\ \mathbf{J}_k{}^{a} \\ \mathbf{M}_k{}^{i} \\ \mathbf{J}_k{}^{i} \end{bmatrix} \\
&\qquad = \begin{Bmatrix} \epsilon_e [-\hat{\mathbf{n}}_1 \times (\mathbf{E}_{\mathrm{inc}} + \mathbf{E}_{\mathrm{ref}})] \\ \mu_e [\hat{\mathbf{n}}_1 \times (\mathbf{H}_{\mathrm{inc}} + \mathbf{H}_{\mathrm{ref}})] \end{Bmatrix}. \quad (19)
\end{aligned}
$$

In Eq. (19) the superscripts a and i represent the actual and the image sources, respectively, the subscript k represents the kth tangential component ($k = 1, 2$) in the local coordinate system, and ($\mathbf{M}_k{}^{a}$, $\mathbf{J}_k{}^{a}$), ($\mathbf{M}_k{}^{i}$, $\mathbf{J}_k{}^{i}$) represent the current density vectors on the top and bottom scatterer, respectively, at each node. The submatrices $\mathbf{A}_{ij}$ are obtained first by substitution of Eqs. (16)–(18) into Eqs. (14) and (15), which transforms the continuous current densities $\{\vec{M}, \vec{J}\}$ into a set of discrete current densities defined only at the nodes. Next these unknown nodal current densities are factored out of the integrand, and the remaining terms of the integrand are then in-

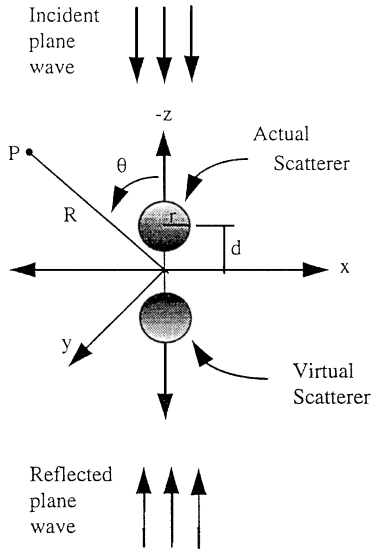

Fig. 4. Test configuration for the problem of a spherical scatterer above a perfectly conducting half-space. The differential scattering cross section is calculated as a function of θ in the $y-\,-z$ plane. The incident wave is a unit-amplitude plane wave polarized in the $+y$ direction, traveling in the $+z$ direction.

tegrated numerically with general quadrature methods. Results of these integrals are placed in the coefficient matrices $\mathbf{A}_{ij}$ and are used for solving the unknown nodal current densities. For example, $\mathbf{A}_{11}$ represents the sum of free terms 1 and 6 and integral terms 2 and 7, $\mathbf{A}_{12}$ represents the sum of integral terms 3 and 8, $\mathbf{A}_{13}$ represents integral term 4, and $\mathbf{A}_{14}$ represents integral term 5 on the left-hand side of Eq. (14). Similarly, row 2 of the coefficient matrix $\mathbf{A}$ is obtained from Eq. (15). The size of the submatrix $\mathbf{A}_{ij}$ is $(2N \times 2N)$, and the size of each of the current-densities vector $(\mathbf{M}_k{}^i, \mathbf{J}_k{}^i)$ and $(\mathbf{M}_k{}^a, \mathbf{J}_k{}^a)$ is $(4N \times 1)$, where N is the number of nodes on each of the two scatterers. The factor of 4 comes from the fact that there are N nodes on each scatterer, and every node contains 2 vector current densities each with 2 tangential components. The number of nodes on the top scatterer must be equal to the number of nodes on the bottom scatterer, because with each actual source present there must exist a corresponding imaged source as imposed by IT. Equation (19) is an underdetermined system, with only $4N$ equations but $8N$ unknowns. To make Eq. (19) uniquely solvable, we apply the Cartesian component relations between the actual node currents and their corresponding image nodal currents,

$$J_x{}^a = -J_x{}^i, \tag{20}$$

$$J_y{}^a = -J_y{}^i, \tag{21}$$

$$J_z{}^a = J_z{}^i, \tag{22}$$

$$M_x{}^a = M_x{}^i, \tag{23}$$

$$M_y{}^a = M_y{}^i, \tag{24}$$

$$M_z{}^a = -M_z{}^i, \tag{25}$$

to obtain a $(4N \times 4N)$ system,

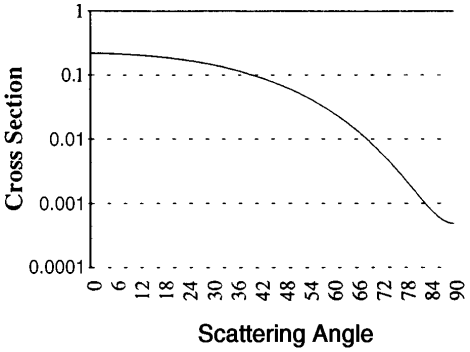

Fig. 5. Differential scattering cross section of a sphere on a perfectly conducting half-space, with $r = 0.2$, $d = 0.2$, index of refraction $N = 1.46$.

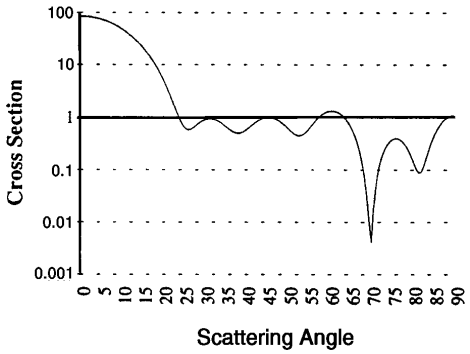

Fig. 6. Differential scattering cross section of a sphere on a perfectly conducting half-space, with $r = 1.0$, $d = 1.0$, index of refraction $N = 1.46$.

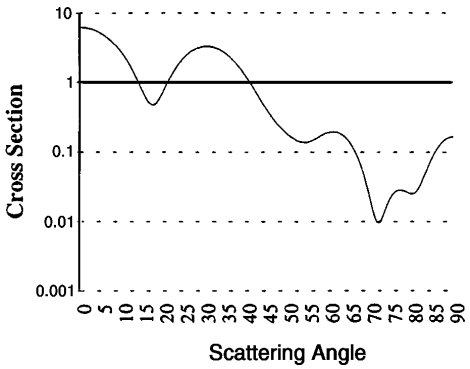

Fig. 7. Differential scattering cross section of a sphere on a perfectly conducting half-space, with $r = 1.0$, $d = 1.0$, index of refraction $N = 1.30$.

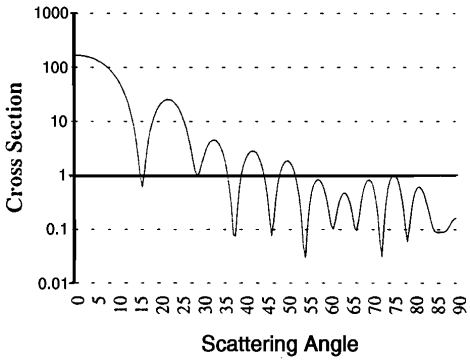

Fig. 8. Differential scattering cross section of a sphere on a perfectly conducting half space, with $r = 1.0$, $d = 5.0$, index of refraction $N = 1.30$.

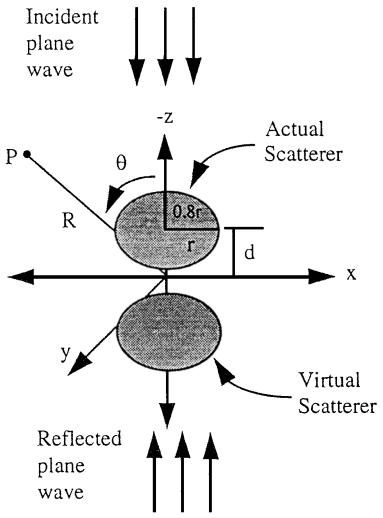

Fig. 9. Simulation of an ellipsoid above a perfectly conducting half-space. The differential scattering cross section is calculated as a function of θ in the $y-\,-z$ plane. The incident wave is a unit-amplitude plane wave polarized in the $+y$ direction, traveling in the $+z$ direction.

$$\begin{bmatrix} (\mathbf{A}_{11} \pm \mathbf{A}_{13}) & (\mathbf{A}_{12} \pm \mathbf{A}_{14}) \\ (\mathbf{A}_{21} \pm \mathbf{A}_{23}) & (\mathbf{A}_{22} \pm \mathbf{A}_{24}) \end{bmatrix} \begin{bmatrix} \mathbf{M}_k{}^a \\ \mathbf{J}_k{}^a \end{bmatrix} = \begin{Bmatrix} \epsilon_e[-\hat{\mathbf{n}}_1 \times (\mathbf{E}_{\text{inc}} + \mathbf{E}_{\text{ref}})] \\ \mu_e[\hat{\mathbf{n}}_1 \times (\mathbf{H}_{\text{inc}} + \mathbf{H}_{\text{ref}})] \end{Bmatrix}, \quad (26)$$

and the actual current densities ($\mathbf{M}_k{}^a$, $\mathbf{J}_k{}^a$) can be solved. Then one can calculate ($\mathbf{M}_k{}^i$, $\mathbf{J}_k{}^i$) from these actual sources by applying Eqs. (20)–(25). Finally, to solve for the scattered electric fields $\vec{E}_{\text{sca}}$ in the external region, one simply substitutes the calculated current densities ($\mathbf{M}_k{}^i$, $\mathbf{J}_k{}^i$) and ($\mathbf{M}_k{}^a$, $\mathbf{J}_k{}^a$) into Eq. (1). An attractive feature of the BIE method is that for a fixed scatterer position, one would need to invert the coefficient matrix only once. Any subsequent change in the incident fields would require only a simple backsubstitution step in order to produce the new surface solution.

4. NUMERICAL RESULTS

The configuration for the test problem is shown in Fig. 4, where a single dielectric sphere is suspended at a distance d above the perfectly conducting half-space. The radius of the sphere, r, is expressed in terms of the incident wavelength λ. The incident field is a unit-amplitude plane wave polarized in the y direction. The scattered fields are calculated in the far-field region and expressed in terms of the differential cross section[2] C_{sca} in the $y-\,-z$ plane as a function of the scattering angle θ. The differential cross section is computed with Eq. (27):

$$C_{\text{sca}} = \frac{R^2|\vec{E}_{\text{sca}}(R)|^2}{|\vec{E}_{\text{inc}}|^2}, \quad (27)$$

where R is the distance between the field point P and the origin. It has been our experience that, typically, it takes approximately 3 or 4 elements per free-space wavelength in each dimension to discretize the scatterer adequately. In this test each sphere is consistently discretized into 80 conforming elements[16]: 8 triangular elements on each of the two poles and 64 quadrilateral elements on the remaining surface, for a total of 222 nodes on each sphere for convenience. Consequently, the coefficient matrix has dimensions of 888×888. Each entry in the matrix is a single precision complex number. Therefore it requires roughly 3 Mbytes of memory to store the matrix. This memory requirement is moderate, considering the large amount of memory present on a typical workstation. All of our computations were done in DEC/AXP workstations with an average run time of 8 min per configuration. Furthermore, the same quadratic basis functions are used to interpolate both the geometry information and the unknown density functions.[16] These basis functions are continuous across adjacent elements for all components of the current densities. Therefore there is no artificial charge buildup at the element boundaries. The results are shown in Figs. 5–8 for various separation distances and radii of the spheres. In general the results obtained with the BIE method are in good agreement with the analytical solutions found in Ref. 2, particularly for the maximum differential cross-section values (which typically occur at 0°). There are slight discrepancies between the BIE solutions and the analytical solutions. For example, the differential cross section in Fig. 7 reaches a local minimum at 85°, whereas the analytical solution does not exhibit this behavior. These minor discrepancies occur only at locations where the scattering cross section values are at least several orders of magnitude smaller than the maximum value. This type of numerical error is expected, because the BIE method is a method that employs numerical approxi-

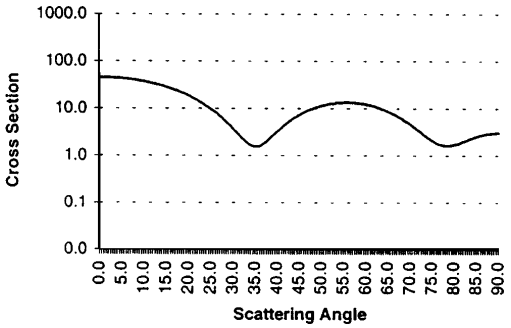

Fig. 10. Differential scattering cross section of an ellipsoid on a perfectly conducting half-space, with $r = 0.5$, $d = 0.5$, index of refraction $N = 1.70$.

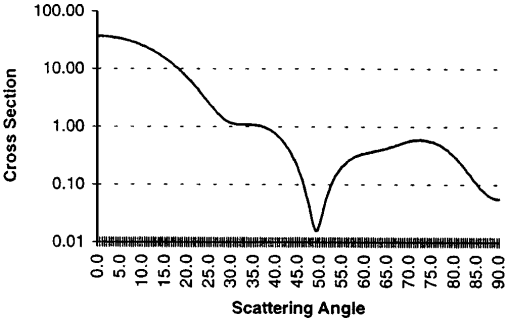

Fig. 11. Differential scattering cross section of an ellipsoid on a perfectly conducting half-space, with $r = 1.0$, $d = 1.0$, index of refraction $N = 1.30$.

mation through the use of basis function expansions. Finally, to simulate the problem of particle contamination, ellipsoidal scatterers that realistically resemble the shape of actual dust particles are considered and are shown in Fig. 9. Each ellipsoid is discretized into 100 conforming elements for a total of 282 nodes. The size of the coefficient matrix is 1128×1128. The differential scattering cross sections as a function of scattering angles for various separation distances and indices of refraction are calculated and plotted in Figs. 10–11.

5. CONCLUSION

A general approach for calculating the EM scattered fields from a dielectric particle near a perfectly conducting half-space impinged upon by arbitrary incident fields is presented. The approach utilizes the boundary integral equation method and exploits the component relationship between actual and virtual sources to reduce the size of the system to be solved. This is identical to a method that uses the modified Green function for a perfectly conducting half-space. The major advantage of using the boundary integral equation method is its ability to solve the EM scattering problem involving arbitrarily shaped scatterers. The results obtained for the cases of spherical and ellipsoidal scatterers, which we expect to be comparably good for other scatterers, are indicative of the effectiveness of this approach.

*Present address, University of Manchester, Manchester, UK.

REFERENCES

1. R. P. Young, "Low scatter mirror degradation by particle contamination," Opt. Eng. **15,** 516–520 (1976).
2. B. R. Johnson, "Light scattering from a spherical particle on a conducting plane: I. Normal incidence," J. Opt. Soc. Am. A **9,** 1341–1351 (1992).
3. G. Videen, "Light scattering from a sphere on or near a surface," J. Opt. Soc. Am. A **8,** 483–489 (1991).
4. P. A. Bobbert and J. Vlieger, "Light scattering by a sphere on a substrate," Physica A **137,** 209–242 (1986).
5. I. V. Lindell, A. Sihvola, K. Muinonen, and P. Barber, "Scattering by small object close to an interface: I. Exact image theory formulation," J. Opt. Soc. Am. A **8,** 472–476 (1991).
6. K. B. Nahm and W. L. Wolfe, "Light scattering models for sphere on a conducting plane: comparison with experiments," Appl. Opt. **26,** 2995–2999 (1987).
7. D. C. Weber and E. D. Hirleman, "Light scattering signatures of individual spheres on optically smooth conducting surfaces," J. Opt. Soc. Am. A **19,** 4019–4026 (1988).
8. W. S. Hall, X. Mao, and W. Robertson, "Quadratic, isoparametric BEM formulation for electromagnetic scattering from arbitrarily shaped three-dimensional homogeneous dielectric objects," in *Boundary Elements XIV,* C. A. Brebbia, J. Dominguez, and F. Parvis, eds. (Computational Mechanics Publications, Southampton, UK, 1992).
9. J. C. Chao, Y. J. Liu, F. J. Rizzo, P. A. Martin, and L. Udpa, "Regularized integral equations and curvilinear boundary elements for electromagnetic wave scattering in three dimensions," IEEE Trans. Antennas Propag. (to be published).
10. J. R. Mautz, "A stable integral equation for electromagnetic scattering from homogeneous dielectric bodies," IEEE Trans. Antennas Propag. **AP-37,** 1070–1071 (1987).
11. E. Marx, "Integral equation for scattering by a dielectric," IEEE Trans. Antennas Propag. **AP-32,** 166–172 (1984).
12. W. C. Chew, *Waves and Fields in Inhomogeneous Media,* 1st ed. (Van Nostrand Reinhold, New York, 1990), Chap. 2, pp. 68–72.
13. C. A. Balanis, *Advanced Engineering Electromagnetics,* 1st ed. (Wiley, New York, 1989), Chap. 7, p. 317.
14. P. A. Martin and P. Ola, "Boundary integral equations for the scattering of electromagnetic waves by homogeneous dielectric obstacles," Proc. R. Soc. Edinburgh A **123,** 185–208 (1993).
15. J. R. Mautz and R. F. Harrington, "Electromagnetic scattering from homogeneous body of revolution," Archiv. Elektronik Übertagungstechnik, **33,** 71–80 (1979).
16. J. C. Chao, "A boundary integral equation approach to three dimensional electromagnetic wave scattering problems," Ph.D. dissertation (Iowa State University, Ames, Ia., 1994).